

# High resolution non-contact thermal characterization of semiconductor devices

James Christofferson<sup>a</sup>, Daryoosh Vashae<sup>a</sup>, Ali Shakouri<sup>\*a</sup>, Philip Melese<sup>\*\*b</sup>

<sup>a</sup>Jack Baskin School of Engineering, University of California at Santa Cruz; <sup>b</sup>SRI International

## ABSTRACT

Non-contact optical methods can be used for sub micron surface thermal characterization of active semiconductor devices. Point measurements were first made, and then real time thermal images were acquired with a specialized PIN-array detector. This method of thermal imaging can have spatial resolution better than the diffraction limit of an infrared camera and can work in a wide range of ambient temperatures. The experimentally obtained thermal resolution is on the order of 50mK.

Key words: Thermal Imaging, Thermoreflectance, Semiconductor Imaging,

## 1. INTRODUCTION

With advances in fabrication techniques, semiconductor devices become smaller, faster and also hotter. Effective thermal management will be essential for the reliability of small and fast semiconductor devices in the near future. Thus, the study and characterization of thermal effects on the scale of these devices is important.

The thermoreflectance technique provides a relatively cheap and easy way to obtain thermal measurements on semiconductor devices with excellent spatial and thermal resolution. Furthermore, this method can be extended to do surface temperature mapping with the use of an area detector and parallel processing of the data. This thermoreflectance microscope can create quantitative, real time thermal images with better spatial resolution than is possible with the 3 micron diffraction limit of commercially available infrared microscopes.

Also, since the thermoreflectance technique does not rely upon the emitted black body radiation of the sample, low temperature thermal measurements are possible. For example, thermoreflectance imaging may be the only non-contact way to measure the temperature on an active semiconductor device in a cryostat.

### 1.1 Previous thermoreflectance experiments

Goodson<sup>1</sup> experimented on metal interconnects similar to the experiments of Quintard<sup>2</sup> and Claeys<sup>3</sup>. The thermoreflectance

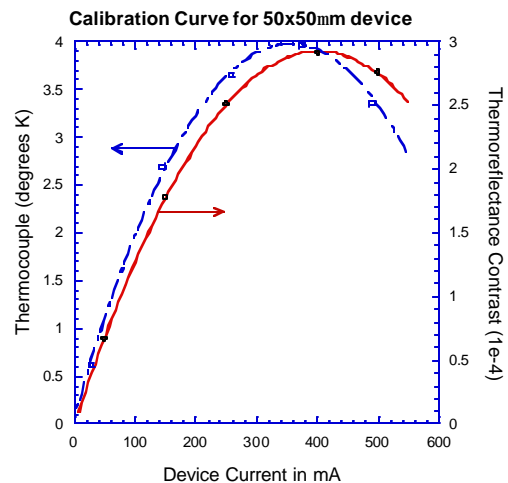


Figure 1: Comparison of thermoreflectance probe and thermocouple on micro-cooler surface

\* Corresponding author: [ali@cse.ucsc.edu](mailto:ali@cse.ucsc.edu); phone (831) 459-3821; <http://www.cse.ucsc.edu/~ali>; UC Santa Cruz, 1156 High, Santa Cruz Ca 95064

\*\* [philip.melese@sri.com](mailto:philip.melese@sri.com), SRI International, Menlo Park, Ca 94025-3493

signal was calibrated with thermistor measurements. These experiments are measuring a temperature change of 10's of degrees and they focused on the transient response. We need to be 100 times more sensitive! We will see that this can be accomplished with heterodyne filtering as discussed by Batista<sup>4</sup> who measured the heating on a 35x35 micron MOS transistor, and Mansanares<sup>5</sup> who measured temperature in a semiconductor laser. Our experiments show that one can achieve both high spatial and thermal resolution, and also generate real time thermal images.

### 1.2 Surface thermal measurements on active micro-coolers

Experiments were performed on thermionic micro coolers<sup>6,7</sup> ranging in size from 10x10 micron to 130x130 micron. Micro coolers provide an excellent test platform because of the interesting thermal profile.

Previous experimental measurements of the device temperature were done in the lab by using a micro thermocouple in contact with the device. The smallest thermocouple available is about 50µm in diameter. A comparison of the thermocouple results and the thermoreflectance signal is shown in figure 1 along with the quadratic fit. We see a maximum cooling of about 4 degrees at about 280mA. Using this plot, we can calibrate the thermoreflectance coefficient of the surface.

## 2.EXPERIMENTAL SETUP

The experimental setup is rather simple and is shown in figure 2. Incident white light from a fiber optic illuminator is incident on the thermally modulated sample through a beam splitter and the reflected, enlarged image is incident on the detector. For point measurements, a silicon photodiode with a pinhole was used. For thermal imaging, the photodiode was replaced with the PIN-array detector.

The signal from the photodiode is amplified and processed by a lock-in amplifier. A lock-in amplifier is used for its superior noise filtering, on the small thermoreflectance signal. Because there is a need for high spatial resolution, the amount of light that is reflected off of a small area is slight and the thermoreflectance signal is even smaller. For an area corresponding to 10µm<sup>2</sup> we have about 1µA photocurrent, of which only 10pA is the modulated thermoreflectance signal. The thermal resolution is dictated by the amount of thermal signal compared to the fundamental shot, and Johnson noise.

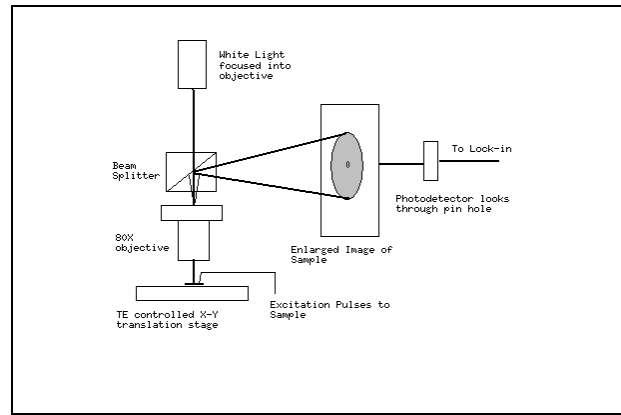


Figure 2: Experimental Setup.

### 2.1 Thermal reflectance measurement

It is known that the reflection coefficient has a small linear dependence on temperature. The normalized change in reflection per unit temperature is called the thermoreflectance constant and is denoted by  $C_{th}$ .

$$C_{th} = (1/R)(dR/dT)$$

$C_{th}$  is 1.5e-4 for silicon and around 1e-5 for metals.

Because of the small temperature dependence of the reflection coefficient we must modulate the temperature use lock-in technique. We excite the sample with a current pulse, and as long as the excitation period is long enough for the device to reach thermal equilibrium, the magnitude of the flicker seen at the detector at the excitation of the frequency is proportional to the change in temperature.

Let the reflection coefficient of the sample be the initial reflection coefficient at ambient,  $R_0$ , plus the change from a change in temperature.

$$R(T) = R_0 + dR/dT * \Delta T$$

Let  $P_{ref}$  be the power reflected of the sample, and acquired by the photo detector, and  $P_{in}$  be the optical power incident on the sample.

$$P_{ref} = P_{in} * (R_0 + dR/dT * \Delta T)$$

$$P_{ref} = P_{in}R_0 + P_{in} dR/dT * \Delta T$$

Let us assume that  $\Delta T$  is periodic at some excitation frequency  $\omega$ . Let  $P_\omega$  be the power at the excitation frequency that we recover through filtering.

$$P_\omega = P_{in} * dR/dT * \Delta T$$

And recalling the definition of the thermorefectance constant

$$C_{th} = 1/R_0 * dR/dT$$

Thus the change in temperature is

$$\Delta T = P_\omega / (P_{in} * R_0 * C_{th})$$

But  $P_{in} * R_0$  is simply the unmodulated, DC reflectivity of the sample. Therefore, the experimentally obtained change in temperature is the lock-in signal divided by the normalization, which is the DC magnitude, times the thermorefectance constant.

From the above calibration in figure 1,  $C_{th}$  for our white light source and the gold surface is about  $8e-5$ .

## 2.2 Experimental Results

Point measurements can give important insight as to the performance of the coolers that are too small to be measured by the thermocouple. However, we can also scan the cooler to learn more about the behavior of the cooler so that the design can be improved. Figure 3 shows the geometry of the sample to be scanned, and figure 4 shows the results of a scan from the current probe to the cooler down the contact layer for different bias currents. We see that there is heat generated at the probe, then cooling at the surface of the cooler.

## 3. THERMOREFLECTANCE IMAGING

Previous experiments have attempted to acquire thermorefectance images, by using a traditional CCD, then performing image processing on the images that are acquired. In particular, experiments by Grauby<sup>8</sup> and also Spirig<sup>9</sup> show that such experiments are possible. However, in these experiments, the thermal images are only sensitive to 10's of degrees of temperature change. After some study, we found that it is impossible to use a currently available CCD camera to recover the thermorefectance signal with resolution of .1 degrees. Quite simply CCD's don't have enough dynamic range for our application.

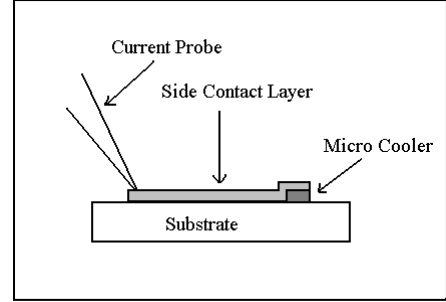


Figure 3: Geometry of micro-cooler samples.

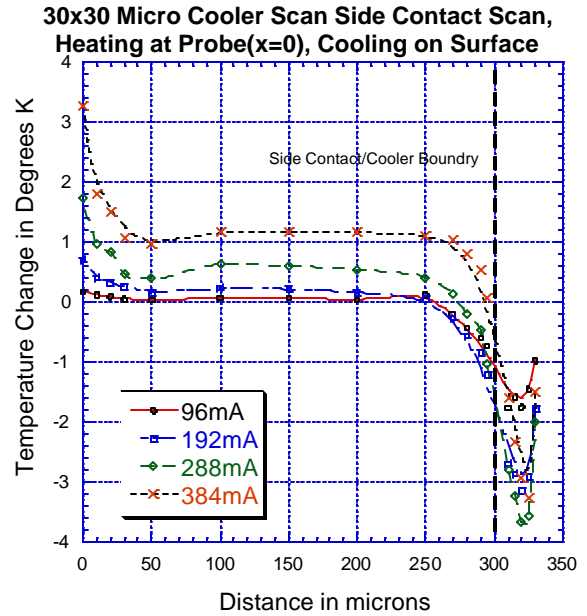


Figure 4: Temperature distribution of micro-cooler and contact layer.

A specialized camera with a large dynamic range is being developed by Philip Melese at SRI International. This camera can capture AC images up to 512Hz. The camera uses a 16x16 photodiode array, with active amplifiers at each pixel.

### **3.1 Signal processing required to acquire the thermal Image**

Several processing steps have to be taken before the thermal image can be realized. They are filtering, normalization, recovery of phase image, and correcting for different thermorefectance constants of reflection surfaces.

Because of the small magnitude of the thermorefectance signal, we must take a fast fourier transform at each pixel then look at the signal at our excitation frequency. This takes the place of the lock-in filtering for the point measurements. This can be done in real time with a 1Hz bandwidth by the data acquisition computer. In the images presented, the FFT is performed with a .033 Hz bandwidth window for each pixel, which greatly reduces the noise.

From the above equations, we know that the temperature change is proportional to the magnitude of the light at the cycling frequency divided by the DC light for each pixel, however, a correction must be made for the different reflection surfaces. Each surface will have a different thermorefectance coefficient. The thermal image is the micro cooler top surface, of gold, but there is also the surrounding area of the substrate. The Si substrate has a fairly well known thermorefectance constant of  $1.5e^{-4}$ . Thus, we can determine which points are on the silicon and correct for that factor. One way to determine the different reflection surfaces is to look at the histogram of the image. In this study, there are only two reflection surfaces, the substrate, and the gold layer. Since these materials have different overall reflectivity, the data points off each surface can be determined by looking at the histogram of the image. The histogram should be bi-modal, indicating the silicon, and gold points.

Finally, we must correct for the points that are heating or cooling. It is fairly easy to obtain the magnitude of the signal at the cycling frequency, but the sign of the signal is not easily known. By identifying the phase of the signal, the cooling and heating points can be determined. This problem is exacerbated by the problem that the 256 pixels are not exactly read in parallel. There is a slight delay from each channel on each data acquisition board.

To process the image we can generate a mask, from the above steps, and then multiply the mask with the unprocessed image. Figure 6 shows the mask that was generated for the 20x20 micro-cooler image. Three regions are identified, the black represents the data points off gold that are cooling, the white represents the data points off gold that are heating, and the gray are the points that reflect off the silicon. The computer generated mask is not perfect. For example there is some background light leaking into the image around the edges, which the computer considers as a gold surface. In practice, we run the computer algorithm as described above, then correct the misinterpretations manually.

In order to view a 'real' time image all of the above steps have to be processed quickly. The most computationally intense operation is to perform a fast fourier transform on the data to provide enough filtering to see the thermal signal. The other signal processing steps should be fairly quick, but may require some input from the user.

### **3.2 Experimental results from the thermal camera:**

Thermal images were acquired for different size devices at different currents. A CCD image in figure 5 shows a 20x20 micro-cooler. The thermal images represent approximately 2.5 microns per pixel, which is higher resolution than the infrared camera diffraction limit. Figure 7 shows the DC normalization image of the cooler as produced by the 16x16 thermal camera, while in figure 8 we see the processed thermal image. The thermal image shows a nice temperature distribution of cooling across the cooler surface, and a little more than 2 degrees cooling.

These images can be used to identify device fabrication errors. Figure 9 shows the normalization image of a different 20x20 micro cooler. As seen in the thermal image, figure 10, there is less cooling on the surface, and there is a large heating at the junction from the contact layer to cooler. Figure 11, shows a cross section of the thermal image, plotting the device that was fabricated correctly and the device with a fabrication error. This has been identified as joule heating caused by poor deposition of the contact layer.

#### **4.CONCLUSION**

Thermoreflectance images of operating micro coolers are presented with high spatial resolution and 50mK thermal resolution. Work progressed from a point measurement to a scan to finally a thermal image acquired in 'real time' with a high dynamic range, AC coupled camera. Several images are presented that have better spatial resolution than a diffraction limited infrared camera. The main drawback in thermoreflectance imaging is in the uncertainty in calibration, which has to be done with a thermocouple. However, this is comparable to emissivity calibration problems in infrared camera systems. Further optimization of the sensor, optics, and signal processing will result in an extremely good thermal microscope. We expect spatial resolution below one micron and temperature sensitivity on the order of 10mK should be achievable.

#### **ACKNOWLEDGMENTS**

We would like to thank Ed Croke for the molecular beam epitaxy growth and also Xiofeng Fan and Gehong Zheng for the fabrication of the cooler samples used in this experiment. This work was funded by the Packard Foundation and DARPA Heretic program.

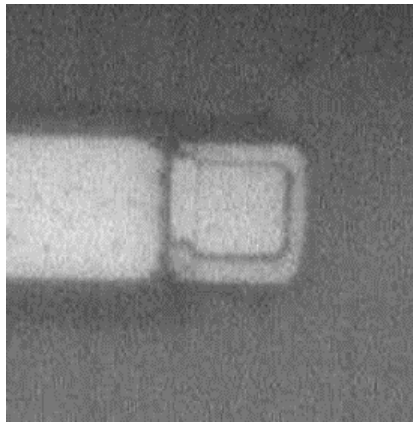


Figure 5: CCD image of 20x20 micro-cooler.

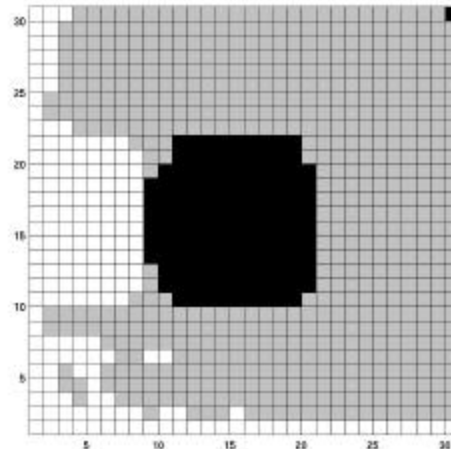


Figure 6: Computer generated mask identifying 3 regions.

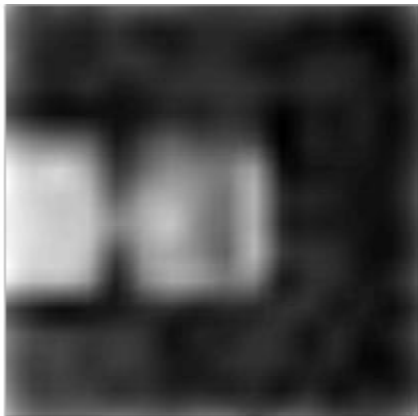


Figure 7: Normalization image of 20x20 micro-cooler.

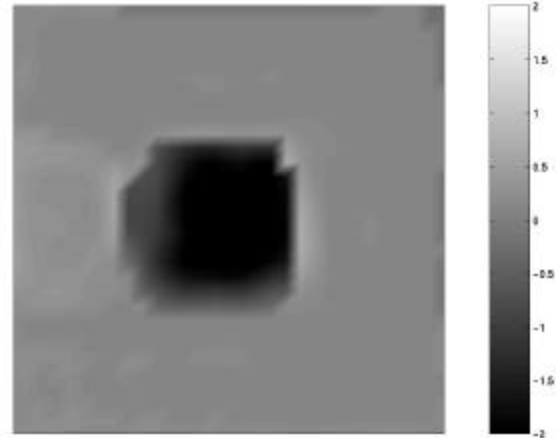


Figure 8: Thermal image showing good cooling distribution.

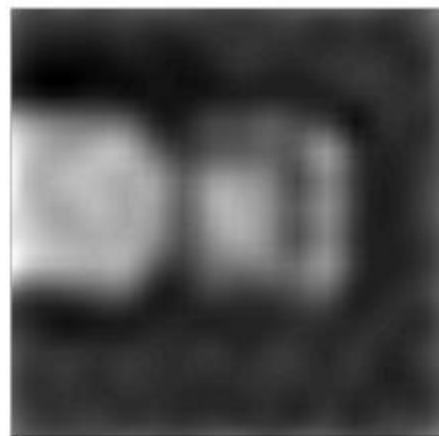


Figure 9: Normalization image of cooler with fabrication error.

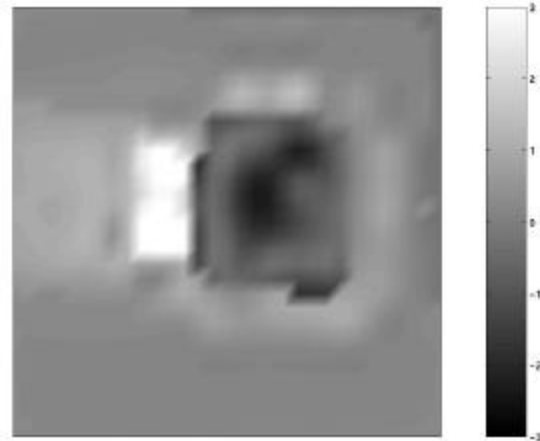


Figure 10: Thermal image showing excessive Joule heating due to fabrication error.

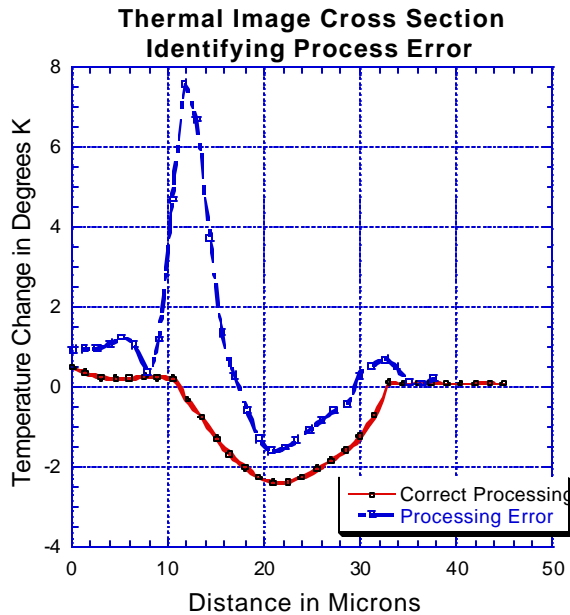


Figure 11: Thermal image cross-section comparison of two 20x20 devices.

## REFERENCES

1. K.E. Goodson and Y.S. Ju, "Short-time-scale thermal mapping of microdevices using a scanning thermoreflectance technique," *Trans. of the ASME*, p.306-313, May 1998.
2. Quintard, Dilhaire, Phan, and Claeys. "Temperature measurement of metal lines under current stress by high resolution laser probing," *IEEE Trans. on Instrumentation and Measurement*, p.69-74, Feb 1999.
3. T Phan, S Dilhaire, V Quintard, W Claeys, and J Batsale. "Thermoreflectance measurements of transient temperature upon integrated circuits: application to thermal conductivity identification," *Microelectronics Journal*, 29:181-190, 1998.
4. J. Batista, A Mansanares, EC DaSilva, M Pimentel, N Januzzi, D Fournier. "Subsurface microscopy of biased metal oxide semiconductor field effect transistor structures: photothermal and electroreflectance images," *Sensors and Actuators A*, 71:40-45, 1998.
5. A Mansanares, D Fournier, A Boccara. "Temperature measurements of telecommunication lasers on a micrometre scale", *Electronics Letters*, 29(23):2045-2047, 1993.
6. Ali Shakouri and John E. Bowers, "Heterostructure Integrated Thermionic Coolers", *Applied Physics Letters*, 71(9), pp. 1234-1236, September 1997.
7. Gehong Zeng; Shakouri, A.; Bounty, C.L.; Robinson, G.; Croke, E.; Abraham, P.; Xiaofeng Fan; Reese, H.; Bowers, J.E. "SiGe micro-cooler," *Electronics Letters*, vol.35 (24), 25:2146-7, Nov. 1999..
8. S Grauby, S Hole and D Fournier. "High resolution photothermal imaging of high frequency using visible charge couple device camera associated with multichannel lock-in scheme," *Review of Scientific Instruments*. P.3603-3608, Sept.1999.
9. T Spirig, P Seitz, O Vietze, and F. Heitger. "The lock in ccd, two dimensional synchronous detection of light," *IEEE Journal of Quantum Electronics*, p.1705-1708, Sept. 1995.